

Micromechanisms of Thermomechanical Fatigue—A Comparison With Isothermal Fatigue

(NASA-TM-87331) MICROMECHANISMS OF
THERMOMECHANICAL FATIGUE: A COMPARISON WITH
ISOTHERMAL FATIGUE (NASA) 21 P
HC A02/MF A01

N86-28164

CSCL 11F

G3/26

Unclass
43362

Robert C. Bill
Propulsion Directorate
U.S. Army Aviation Research and Technology Activity—AVSCOM
Lewis Research Center
Cleveland, Ohio

Prepared for the
International Spring Conference "Fatigue at High Temperatures"
sponsored by the Societe Francaise de Metallurgie
Paris, France, June 9-11, 1986



MICROMECHANISMS OF THERMOMECHANICAL FATIGUE -
A COMPARISON WITH ISOTHERMAL FATIGUE

Robert C. Bill
Propulsion Directorate
U.S. Army Aviation Research and Technology Activity - AVSCOM
Lewis Research Center
Cleveland, Ohio 44135

SUMMARY

Thermomechanical Fatigue (TMF) experiments were conducted on Mar-M 200, B-1900, and PWA-1480 (single crystal) over temperature ranges representative of gas turbine airfoil environments. The results were examined from both a phenomenological basis and a micromechanistic basis. Depending on constituents present in the superalloy system, certain micromechanisms dominated the crack initiation process and significantly influenced the TMF lives as well as sensitivity of the material to the type of TMF cycle imposed. For instance, high temperature cracking around grain boundary carbides in Mar-M 200 resulted in short in-phase TMF lives compared to either out-of-phase or isothermal lives. In single crystal PWA-1480, the type of coating applied was seen to be the controlling factor in determining sensitivity to the type of TMF cycle imposed, out-of-phase lives being shortened compared to in-phase or isothermal lives if a coating that is brittle at the low temperature end of the cycle were applied. Micromechanisms of deformation were observed over the temperature range of interest to the TMF cycles, and provided some insight as to the differences between TMF damage mechanisms and isothermal damage mechanisms. Finally, the applicability of various life prediction models to TMF results was reviewed. It was concluded that current life prediction models based on isothermal data must be modified before being generally applicable to TMF.Doc.

INTRODUCTION

Background

Currently used methods of life prediction and material constitutive modeling for high-temperature gas turbine components usually are based on isothermal data. In reality these components are subjected to both temperatures and mechanical strains that vary with time. Throughout cyclic exposure the microstructure of the material may never reach an equilibrium state. Also, there are no extensive experimental bases for estimating nonisothermal cyclic damage accumulation and material constitutive behavior. Indeed, the integrated effects of damage accumulated over a temperature range are virtually unexplored.

Conditions under which a material specimen is subjected to both temperatures and mechanical strains that vary cyclically constitute what is known as thermomechanical fatigue (TMF). Thermal fatigue experimental evaluations (refs. 1 and 2) incorporate some of the effects present in thermomechanical fatigue but suffer from the drawback that the thermal cycle and the mechanical cycle are inevitably coupled in such a manner that cycle parameters cannot be controlled with any degree of independence.

Developing life prediction capabilities that are directly applicable to nonisothermal situations requires a data base in which temperature and mechanical strain are both independently controlled as a function of time. On this basis it is possible, in principle, either to adapt existing isothermal life prediction methods to TMF or to develop new life prediction methods.

Review of TMF Literature

Some TMF studies performed on various materials are cited in order to illustrate general experimental trends and approaches to adapting isothermal life prediction concepts to TMF conditions. Though not an exhaustive literature survey, the cited work provides a perspective from which to view the present work.

Taira et al. (ref. 3) conducted TMF experiments on 1016 carbon steel and AISI 347 stainless steel and compared their results with isothermal data. They found good correlation between TMF lives and isothermal lives determined at the maximum and minimum temperatures associated with the TMF cycle by invoking a "spanning factor" for use in conjunction with a linear damage accumulation rule. In effect, the spanning factor is a proportionality constant based on isothermal lives at the TMF temperature extremes. The approach is not likely to be generally valid when there is strong interaction among the damage mechanisms operating over the temperature range of the TMF cycle. For one thing, the method restricts TMF lives to lie somewhere between the isothermal lives of the temperature extremes, a phenomenon that is not always observed.

Lundberg and Sandstrom (ref. 4) have shown that strainrange partitioning (SRP) concepts might be used for qualitative extrapolation of isothermal life prediction to TMF situations. In particular, thermal fatigue results for Cr-Mo and 18Cr-10Ni steels could be rationalized on the basis of isothermal SRP data. Lundberg and Sandstrom offer a generally applicable cautionary note, however. Their observations and those of Taira are not applicable to cycle conditions (temperature ranges and hold times) over which microstructural changes to the alloy might be expected.

Halford and Manson (ref. 5) have successfully applied SRP to TMF life prediction for AISI 316 stainless steel. They point out that AISI 316 stainless steel is a material whose basic cyclic strain-life relations are not temperature dependent. Special procedures that have yet to be developed are needed to cope with temperature-dependent materials.

Rau, Gemma, and Leverant (ref. 6) investigated crack propagation under in-phase (maximum tensile strain simultaneous with maximum temperature) and out-of-phase (maximum compressive strain simultaneous with maximum temperature) TMF cycling, as well as under isothermal cycling conditions for some nickel-based superalloys. Crack propagation rates were observed to be much higher for out-of-phase cycling than for in-phase cycling. Also, crack propagation rates under TMF conditions were higher than under comparable (mechanistically) isothermal cycling conditions. A compressive-creep-assisted crack sharpening mechanism was proposed, but not verified, to account for rapid out-of-phase crack propagation.

Kuwabara, Nitta, and Kitamura (ref. 7) investigated the TMF behavior of a broad range of steels and superalloys used in the power generating industry. They observed four distinct types of TMF behavior, each defined by the particular life versus cyclic strain characteristics associated with in-phase and out-of-phase cycling. A conclusion they reached was that 3 of the 4 types of behavior could be conservatively handled by presently available cyclic strain based relationships. The "dangerous" 4th type of TMF behavior was that for which in-phase lives were substantially shorter than out-of-phase or isothermal lives. Kuwabara et al. attributed this fourth type of behavior to substantial creep-fatigue interaction, and noted that it was observed most typically in the cast superalloys they evaluated.

Objective and Scope

There are three objectives to this paper: 1) To observe the effect that TMF cycling has on crack initiation and crack propagation lives of some nickel base superalloys; 2) to identify the important micromechanisms controlling deformation and damage under TMF conditions; 3) to assess the applicability of isothermal life prediction models to TMF.

MATERIALS

The nominal compositions of all three nickel based superalloys of concern in this paper are summarized in table I. A description of the two types of coatings applied to the single crystal PWA-1480 is included in table II.

MAR-M 200 is a cast nickel-based superalloy originally developed for turbine blade application. The microstructure consists of approximately 60 vol % primary γ' in a γ matrix, with both $M_{23}C_6$ and MC type carbides. The alloy was conventionally cast into specimens, resulting in a radial grain structure with grain sizes of approximately 1 mm by 2 to 3 mm. The specimens were tested in the as cast and machined condition.

The B-1900 + Hf referenced in this study is a typical isotropic nickel base superalloy used in gas turbine hot section components such as blades and vanes. Cast bars from which specimens were machined were given a 4 hr. solution treatment at 1079 °C, air cooled, then precipitation treated at 899 °C for 10 hr and air cooled. Resulting grain size was 0.18 to 0.25 mm.

Single crystal PWA-1480 specimens were cast from remelt stock by a directional solidification method wherein the melt-filled mold was withdrawn from a furnace at a rate of about a half centimeter per minute. Using this method, growth direction crystallographic orientation was usually within 5° of $\langle 001 \rangle$.

After casting, the bars were solution heat treated and subjected to visual, x-ray diffraction, and metallographic inspection. Specimens were machined to final configuration from the cast single crystal blanks, following heat treatment and inspection.

EFFECT OF TMF CYCLING ON CRACK INITIATION LIFE

MAR-M 200

The TMF results for MAR-M 200 are summarized in figure 1. The inelastic mechanical strain range is plotted versus the number of cycles to failure. Results are shown for in-phase and out-of-phase TMF experiments as well as isothermal fatigue data at 1000, 927, and 650 °C. A few observations are immediately noteworthy. First, there was a marked sensitivity of TMF life to the type of cycle imposed. The life of polycrystalline MAR-M 200 was considerably shorter under in-phase cycling conditions than under out-of-phase cycling conditions. The significance of the apparent difference in slope between the in-phase and out-of-phase life lines is uncertain; additional data are required to substantiate this difference. Second, TMF lives, especially under in-phase cycling conditions, were considerably shorter than isothermal lives at 1000 and 927 °C. Third, for a given inelastic strain range, the isothermal life showed a notable sensitivity to temperature. However, the isothermal LCF life of MAR-M 200 appeared to be relatively insensitive to the type of isothermal cycle imposed; i.e., the inclusion of hold times did not result in significant changes in cyclic fatigue life. At 927 °C for example, a CC test lasting over 1000 hr had a cyclic lifetime no different from PP tests lasting only 0.2 hr. The TMF tests had exposure times at high temperatures that were greater than those for the isothermal PP tests but less than those for the isothermal CC tests. Nevertheless, in-phase TMF cyclic lives were less than isothermal lives. Thus, time at temperature by itself does not appear to be a critical factor from the standpoint of governing cyclic life.

Metallographic examination of MAR-M 200 TMF specimens, after failure, provided some insight regarding the micromechanisms responsible for the TMF cycle phase effects observed. Figure 2 shows that crack initiation and early crack growth differences under in-phase and out-of-phase conditions are related to: 1) the role of oxidation; 2) carbide and carbide/matrix behavior; and 3) the role of grain boundaries.

Some of the important oxidation related TMF effects may be seen in comparing figure 2(a) and (b). It is evident that in-phase cycling (fig. 2(a)) resulted in relatively sharp crack tips and thick oxide build-up on the crack surfaces, suggesting a brittle propagation mechanisms through oxidized tip material, and some wedging action attributed to the oxide on the crack surfaces. In contrast, out-of-phase cycling (fig. 2(b)) resulted in blunt crack tips, suggesting a ductile propagation mechanism, and relatively oxide-free crack surfaces due to crack closure (compression) at elevated temperature.

The TMF cycle dependent carbide and carbide/matrix behavior is shown in figures 2(c) and (d). In-phase cycling (fig. 2(c)) lead to matrix pull-away from the carbide particle. Subsequent link-up of the voids created by the pull-away and propagating cracks often occurred, based on metallographic observations, as shown in figure 3(a). In contrast, cracking through the carbide was often seen after out-of-phase cycling (fig. 2(d)), presumably due to the high tensile stresses associated with tensile deformation at low temperatures. Based on metallographic studies (fig. 3(b)) from failed specimens, it does not appear that these cracked carbides interacted significantly with major propagating cracks.

Finally, the role of grain boundaries under TMF cycling conditions is shown in figure 2(e) and (f). Under in phase cycling, crack growth is predominantly intergranular, with evidence that internal initiation occurs (fig. 2(e)). Out-of-phase cycling results in mixed intergranular and transgranular crack growth, as may be seen in figure 2(f).

On a finer scale, transmission electron microscopy (TEM) reveals temperature dependent dislocation phenomena that might influence crack initiation during TMF. Figure 4, from the work of Milligan and Jayaraman (ref. 8), summarizes significant temperature dependent behavior in single crystal MAR-M 200 subjected to isothermal cycling at two temperature levels. The important observations are: 1) slip band formation on octahedral slip systems at 760 °C; 2) diffuse slip, and the activation of cubic slip systems at 870 °C.

When a specimen is subjected to TMF cycling between two temperature extremes, possible interaction between these very different dislocation distributions and slip systems may be hypothesized. At elevated temperatures, dislocations from the high dislocation density slip bands generated during low temperature deformation can become mobile in addition to the generally disperse slip associated with high temperature deformation. For in-phase TMF cycling, this can give rise to planar slip features and early crack nucleation, normally associated with low temperature deformation. Also, the development of cubic slip at high temperature will lead to a high density of sessile dislocations at the low temperature. Propagating slip through a dense sessile forest results in large numbers of point defects and dipoles, features that might be significant in void nucleation and diffusion assisted mechanisms. Thus, interaction of alien dislocation distributions and systems helps to account for the general degradation of fatigue life in MAR-M 200 under TMF conditions compared to isothermal conditions.

B-1900

The out-of-phase TMF results for B-1900, summarized from the work of Halford and McGaw (ref. 9), with some preliminary in-phase data (small number of specimens, and different material heat) are shown in figure 5 along with isothermal data for comparison. The out-of-phase TMF results and the isothermal results are very close together, and the preliminary in-phase results suggest a TMF cycle phasing effect similar to that seen for MAR-M 200. Fractography generally showed a mixed intergranular-transgranular fracture surface for in-phase specimens, and predominantly transgranular failure for out-of-phase specimens, much as was observed for MAR-M 200. It should be emphasized that the in-phase results shown in figure 5 are tentative and are clustered in the short life regime, so comparisons with longer life tests are risky.

TEM studies conducted on B-1900 specimens by Pelloux and Marchand (ref. 10) show significantly different dislocation densities and arrangements depending on the phasing of the TMF cycling. Dislocation densities were observed to be higher under in-phase than out-of-phase cycling, as may be seen by comparing figure 6(a) with (b). Also, in-phase cycling resulted in more γ' coarsening and higher misfit dislocation density than did out-of-phase cycling. Pelloux and Marchand attribute the increased dislocation density under in-phase cycling to greater ease of cross slip and secondary source activation at high temperatures, because of partial dislocation constriction promoted by the tensile stresses associated with in-phase cycling. The γ' coarsening was promoted

by the low temperature compressive hydrostatic stress state under in-phase cycling, which tended to cancel the tensile anti-phase boundary stresses. It is difficult to see how these differences in flow behavior and flow related microstructure might be related to damage initiation. Perhaps γ' coarsening and rafting promote channeling of slip and localized intensification under in-phase cycling leading to more rapid crack initiation. There is still a need for more definitive TMF initiation life data for B-1900 before a conclusive understanding of cycle phasing effects can be reached.

Single Crystal PWA-1480

Results from TMF testing of single crystal PWA-1480 are shown in figure 7 (ref. 11). Two points are worthy of note in regard to these results. First, in addition to continuous cycling TMF testing, bi-thermal tests were conducted. Second, the single crystal specimens were coated, with two different kinds of coating being investigated.

The effect of cycle type on specimen crack initiation life is strongly dependent on the type of coating present. For out-of-phase TMF testing, coating effects are especially marked.

The diffusion coating tended to generate circumferential cracks whereas the overlay initiated a multitude of small thumbnail-like cracks, as may be seen in figure 8(a) and (b). The concentric cracking of the diffusion coating is not unexpected since its fracture ductility is low at temperatures below 649 °C (1200 °F).

In-phase TMF crack initiation of coated specimens is less distinct. Because the tensile portion of the test occurs at high temperature, the coatings tend to rumple which makes replication difficult. As can best be determined, in-phase testing generates many small cracks early in the fatigue life of the specimen; however, these cracks do not grow nearly as rapidly as those of out-of-phase testing. As a result, the fatigue lives of in-phase TMF tests are significantly longer than those of out-of-phase tests. In fact, the in-phase lives appeared to be at least as long as isothermal lives at 1038 °C. The complete absence of grain boundaries in the single crystal material may account for the relative insensitivity of the material to in-phase testing, as well as to tensile hold times. Note the deleterious effect of high temperature compressive hold in figure 7, especially for diffusion (brittle) coated specimens. The compressive hold effect is consistent with the impact that out-of-phase cycling has on the brittle coated single crystal.

DISCUSSION

In this section, the applicability of several isothermal life prediction models to the present TMF results is considered. Also, the spanning factor concept proposed by Taira et al. (ref. 3) is given consideration. The isothermal life prediction models that are assessed include SRP (ref. 5), the Ostergren model (ref. 12), the Coffin frequency separation model (ref. 13), and Antolovich's oxidation model (ref. 14). Predictions from these models will be compared with results from MAR-M 200 and B-1900. It is not clear how to apply these models to the single crystal PWA-1480 results because of the dominant role played by the coatings.

Consider first the application of the spanning factor concept to the results obtained for polycrystalline MAR-M 200. Following literally the approach outlined by Taira et al. (ref. 3), the calculated TMF life turned out to be about 1000 cycles for 0.1-percent inelastic strain range. The actual TMF life for in-phase cycling was only 58 cycles, and that for out-of-phase cycling was only 425 cycles. It would seem that Taira et al. made the tacit assumption that isothermal lives should be shorter at high temperatures than at low temperatures - an assumption that may be true for certain alloys, but not so for polycrystalline MAR-M 200 and many other superalloys. If one redefines some of the terms used by Taira et al., so that in effect isothermal lives are assumed to be shorter at low temperatures than at high, the predicted TMF life turns out to be about 62 cycles. Although this calculation is in better agreement with the in-phase experimental results, it is in very poor agreement with the out-of-phase experimental results. The difficulties with the spanning factor approach are now clearly apparent. First, the present formulation of the spanning factor does not account for cycle phasing effects, which were found to be very strong for polycrystalline MAR-M 200. Second, it is not clear a priori how to define the isothermal life terms.

Essentially the same difficulties arise when the spanning factor concept is applied to B-1900 as were encountered for MAR-M 200. Both the life levels and phasing effects could not be consistently predicted using the spanning factor concept.

Difficulties were also encountered in attempting to quantitatively apply isothermal SRP data to the TMF results for polycrystalline MAR-M 200 and to the preliminary results for B-1900 because of the significant cycle phase effect. SRP considerations of the phase effect would be based on two aspects but principally on differences in the four SRP life lines at temperatures within the creep range. Since isothermal SRP data available for polycrystalline MAR-M 200 (ref. 15) indicate that at high temperatures the four SRP life lines are quite close together, the observed TMF effect would not be expected. Thus, the other aspect, based on the variation of SRP life relations with temperature (determined either through direct experiment or through estimation using the ductility-normalized SRP relations of ref. 16) should be examined to see if the variation is consistent with the TMF results. Although a rigorous procedure for dealing with continuous temperature variation has yet to be developed, a life calculation based on extreme or boundary conditions could be applied. Such a calculation was used in reference 16 to predict the thermal fatigue life of a Rene 80 gas turbine blade subjected to factory engine testing. Rene 80, like MAR-M 200, exhibits lower fatigue resistance at lower test temperatures. Applying the procedures used in reference 16 to the TMF results for MAR-M 200 resulted in life predictions that contradicted the observed phase effects. Specifically, out-of-phase TMF lives were calculated to be less than in-phase TMF lives, a prediction that is opposite the observed experimental results.

For the case of B-1900, the isothermal SRP tensile hold results do suggest that for the extremely short life regime (10-100 cycles), in-phase cycling may be very damaging. More complete in-phase TMF data is necessary before thorough assessment of correlation between SRP and TMF results can be made.

The formulation of the Ostergren model (ref. 12) that incorporates time-dependent damage effects is expressed as

$$\sigma_T \Delta \epsilon_p N_{fv}^{(k-1)\beta} = C$$

where σ_T is the peak tensile stress; $\Delta\epsilon_p$, the inelastic strain range; N_f , the number of cycles to failure; ν , the cyclic frequency; and $k, \beta(<0)$, and C , temperature-dependent constants. It appears that the Ostergren model would predict in-phase lives to be higher than out-of-phase lives because of the way σ_T is incorporated. If the frequency were partitioned into compression-going and tension-going terms and these terms were somehow normalized with respect to an intrinsic material (microstructural, mechanistic) relaxation time over the TMF cycle temperature span, a working model for TMF might be developed. Such a development effort would require a clear understanding of controlling damage mechanisms, the rate sensitivity of these mechanisms to temperature, and a prudent choice of isothermal life data to define the constants in the present Ostergren model.

The frequency separation model (13) written in the form that includes tension going and compression-going frequency terms is given by

$$N_f = D \Delta\epsilon_p^a \nu_t^b \frac{\nu_c^c}{\nu_t}$$

If instead of tension-going and compression going frequency terms (ν_t and ν_c respectively), time at temperature terms were incorporated and cast in a manner reflecting the relative damage ranking associated with in-phase and out-of-phase TMF cycling, a basis for developing a TMF life prediction model might be provided.

Antolovich's oxidation model (ref. 14) describes surface initiation of microcracks within a growing oxide film. As presently formulated, no feature addressing in-phase or out-of-phase TMF phenomena is included. If the model were to incorporate the reasonable supposition that crack initiation occurs within the film under the low-temperature tensile portion of the TMF cycle after film growth under high-temperature compression, one would expect out-of-phase cycling to be more damaging than in-phase cycling. This behavior is inconsistent with the present results. Perhaps the oxidation model can be reformulated to describe cyclic-oxidation-assisted crack growth due to rapid oxidation of the crack tip material.

CONCLUSIONS

Although TMF phenomena and mechanisms are material system specific, some generalities appear to hold true. Based on the studies examined in this report, the following conclusions are reached:

1. For polycrystalline materials under very high strain range cycling conditions, in-phase TMF cycling appears to be more damaging than out-of-phase due to concentration of damage at grain boundaries;
2. For the single crystal material examined, the coating played a dominant role in crack initiation, with brittle diffusion type coating showing early initiation during out-of-phase cycling;

3. No generally applicable TMF life prediction model presently exists although various isothermal models could be made to work as phenomenological models for specific materials and cycles;

4. The complexities of TMF cycling are due in part to complex interactions between temperature dependent deformation and damage mechanisms, and in part due to environmental (oxidation) related mechanisms.

REFERENCES

1. Bizon, P.T.; Spera, D.A.: Comparative Thermal Fatigue Resistances of Twenty-Six Nickel- and Cobalt-Base Alloys. NASA TN D-8071, 1975.
2. Whittenberger, J.D.; and Bizon, P.T.: Comparative Thermal Fatigue Resistance of Several Oxide Dispersion Strengthened Alloys. Int. J. Fatigue, vol. 3, no. 4, Oct. 1982, pp. 173-180.
3. Taira, S.; Fujino, M.; and Haji, T.: A Method for Life Prediction of Thermal Fatigue by Isothermal Fatigue Testing. Mechanical Behavior of Materials, The Society of Materials Science, Kyoto, Japan, 1974, pp. 257-264.
4. Lundberg, L.; and Sandstrom, R.: Application of Low Cycle Fatigue Data to Thermal Fatigue Cracking. Scand. J. Metall., vol. 11, no. 2, 1982, pp. 85-104.
5. Halford, G.R.; and Manson, S.S.: Life Prediction of Thermal-Mechanical Fatigue Using Strainrange Partitioning. Thermal Fatigue of Materials and Components, ASTM STP-612, ASTM, 1977, pp. 239-254.
6. Rau, C.A., Jr.; Gemma, A.E.; and Leverant, G.R.: Thermal-Mechanical Fatigue Crack Propagation in Nickel- and Cobalt-Base Superalloys Under Various Strain-Temperature Cycles. Fatigue at Elevated Temperatures, A.E. Carden, A.J. McEvily, and C.H. Wells, eds., ASTM STP-520, ASTM, 1973, pp. 166-178.
7. Kuwabara, K.; Nitta, A.; and Kitamura, T.: Thermal-Mechanical Fatigue Life Prediction in High Temperature Component Materials for Power Plant. Advances in Life Prediction Methods, D. A. Woodford and J. R. Whitehead, eds., ASME, 1983, pp. 131-141.
8. Milligan, W.W.; Jayaraman, N.: High Temperature Low-Cycle Fatigue Mechanisms In Single Crystals of Nickel-Based Superalloy MAR-M 200. NASA CR-174739, 1984.
9. Halford, G.R.; McGaw, M.A.; Bill, R.C.; Fanti, P.D.: Bi-Thermal Fatigue, A Link Between Isothermal and Thermomechanical Fatigue. Proceedings of Symposium on Low Cycle Fatigue - Directions For the Future, ASTM, October, 1985.
10. Marchand, N.J.: Thermal-Mechanical Fatigue Behavior of Nickel-Base Superalloys. PhD Thesis, Massachusetts Institute of Technology, 1986.

11. Swanson, G.A.; and Bill, R.C.: Life Prediction and Constitutive Models For Engine Hot Section Anisotropic Materials. AIAA Paper 85-1421, July 1985.
12. Ostergren, W.J.: A. Damage Function and Associated Failure Equations for Predicting Hold Time and Frequency Effects in Elevated Temperature Low Cycle Fatigue. J. Test. Eval., vol. 4, no. 5, Sept. 1976, pp. 327-339.
13. Coffin, L.F.: The Concept of Frequency Separation in Life Prediction for Time-Dependent Fatigue. 1976 ASME-MPC Symposium on Creep-Fatigue Interaction, R.M. Curran, ed., ASME, 1976, pp. 349-364.
14. Antolovich, S.D.; Liu, S.; and Baur, R.: Low Cycle Fatigue Behavior of Rene-80 at Elevated Temperature. Metall. Trans. A, vol. 12, no. 3, Mar. 1981, pp. 473-481.
15. Manson, S.S.; Halford, G.R.; and Oldrieve, R.E.: Relation of Cyclic Loading Pattern to Microstructural Fracture in Creep-Fatigue, NASA TM-83473, 1982.
16. Halford, G.R.; Saltsman, J.F.; and Hirschberg, M.H.: Ductility Normalized-Strainrange Partitioning Life Relations for Creep-Fatigue Life Predictions. Environmental Degradation of Engineering Materials, M. R. Louthan and R. P. McNitt, eds., Virginia Tech. Printing Dept., Virginia Polytechnic Institute and State University, 1977, pp. 599-612.

TABLE I. - NOMINAL COMPOSITION OF NICKEL BASE SUPERALLOYS

	Ni	Co	Cr	Al	Ti	C	Mo	W	Fe	Cb	Ta	Zr	B	Hf
MAR-M 200	Ba1	10.0	9.0	5.0	2.0	0.15	---	12.0	--	1.0	----	0.05	0.015	----
B-1900 + Hf	Ba1	10.0	8.0	6.0	1.0	.11	6.0	----	--	---	4.25	----	.015	1.15
PWA - 1480	BA1	5.0	10.0	5.0	1.5	----	---	4.0	--	---	12.0	----	----	----

TABLE II. - COATING COMPOSITIONS AND PROCESSES

Coating	Type	Composition	Deposition process
PWA 286	Overlay	NiCoCrAlY +Si+Hf	Vacuum plasma Spray
PWA 273	Aluminide (Outward diffusion)	NiAl	Pack cementation

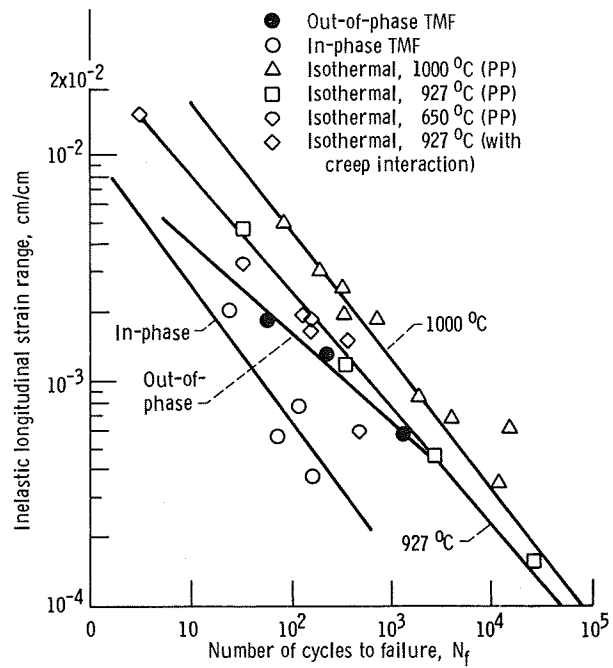
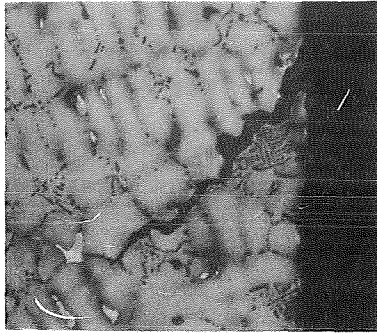
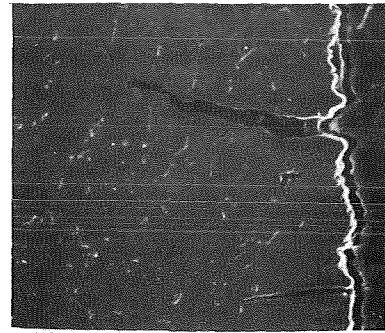


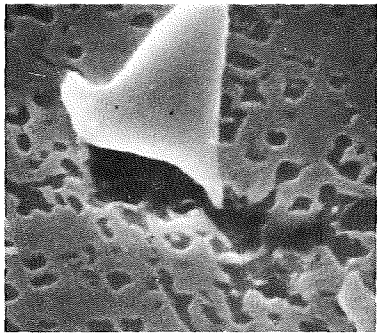
Figure 1. - Isothermal and thermomechanical fatigue results for MAR-M 200 cycled between 500 and 1000 °C.



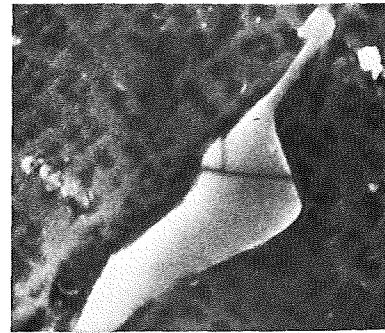
(A) IN-PHASE: NOTE CRACK
TIP AND CRACK SURFACE
OXIDATION.



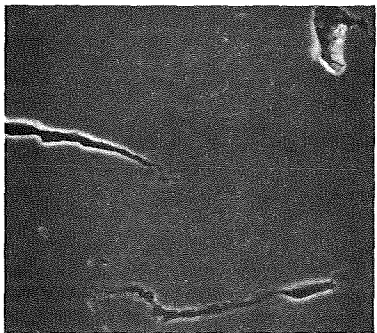
(B) OUT-OF-PHASE: CRACK
TIPS ARE BLUNT AND SURFACES
LESS OXIDIZED.



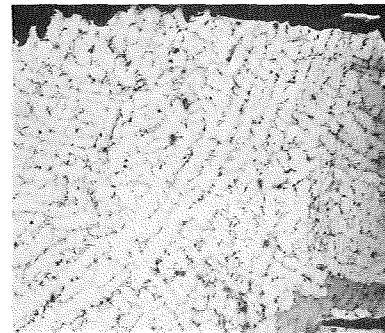
(C) IN-PHASE:
CARBIDE/MATRIX PULL-AWAY.



(D) OUT-OF-PHASE: CRACKING
WITHIN CARBIDES.



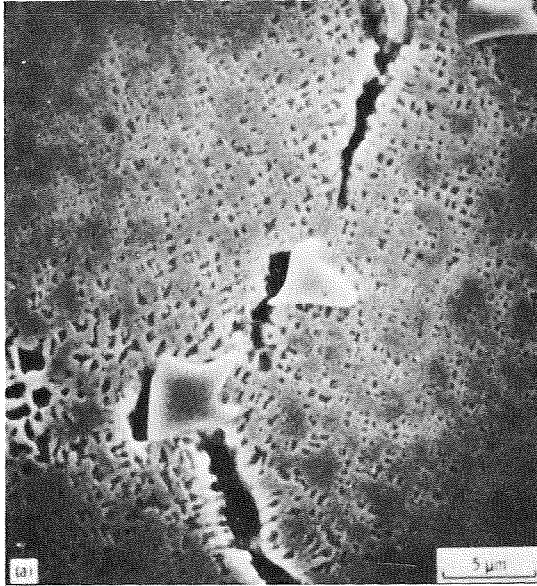
(E) IN-PHASE: INTERGRANULAR
PROPAGATION.



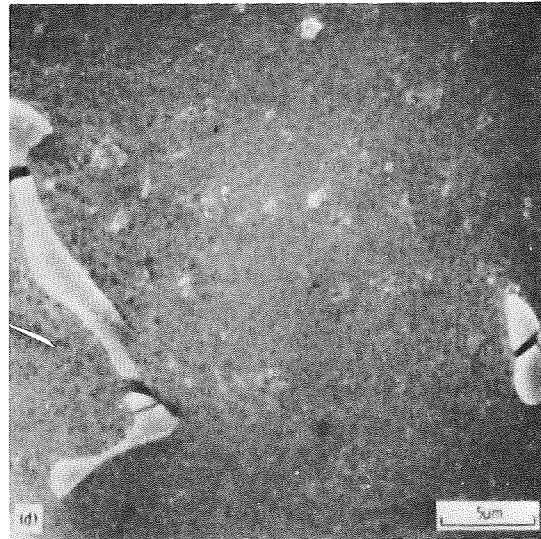
(F) OUT-OF-PHASE:
INTERGRANULAR/TRANSGRANULAR
PROPAGATION.

FIGURE 2.- SOME EFFECTS OF THERMOMECHANICAL FATIGUE CYCLE TYPE ON
MICROMECHANISMS OF CRACK INITIATION AND EARLY PROPAGATION IN
MAR-M 200.

ORIGINAL PAGE IS
OF POOR QUALITY

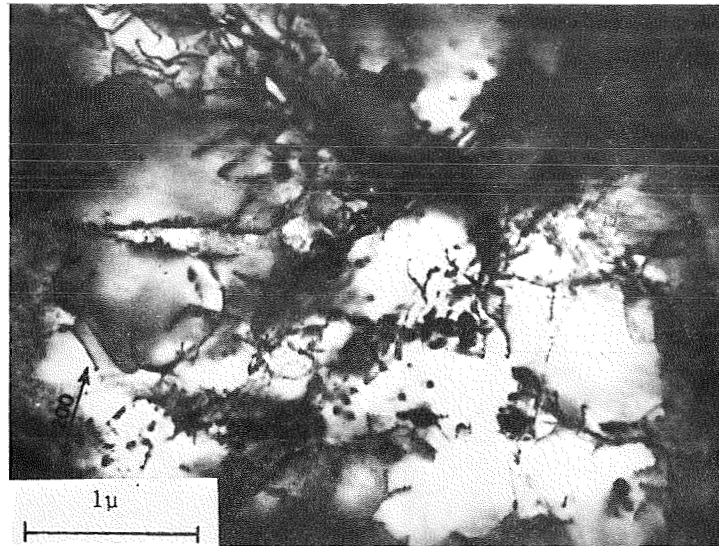


(A) IN-PHASE: CARBIDE/MATRIX PULL-AWAY JOINS WITH GROWING CRACK.

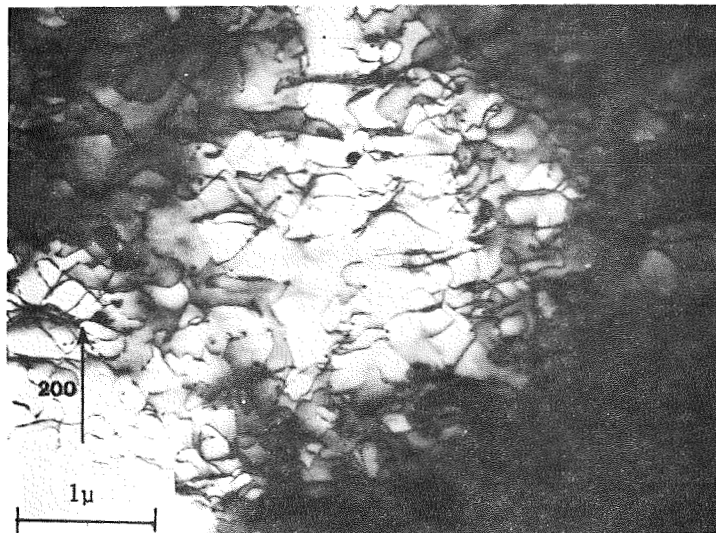


(B) OUT-OF-PHASE: CRACKS WITHIN CARBIDES REMAIN ISOLATED.

FIGURE 3.- ROLE OF CARBIDES IN THERMOMECHANICAL FATIGUE CRACK PROPAGATION IN MAR-M 200.



(A) 760 °C; SLIP BAND FORMATION ON
OCTAHEDRAL SYSTEMS.



(B) 870 °C; DIFFUSE SLIP AND CUBIC
SLIP ACTIVITY.

FIGURE 4.- TEMPERATURE DEPENDENT
MICROSLIP MECHANISMS IN MAR-M 200
(MILLIGAN AND JAYARAMAN, REF.8).

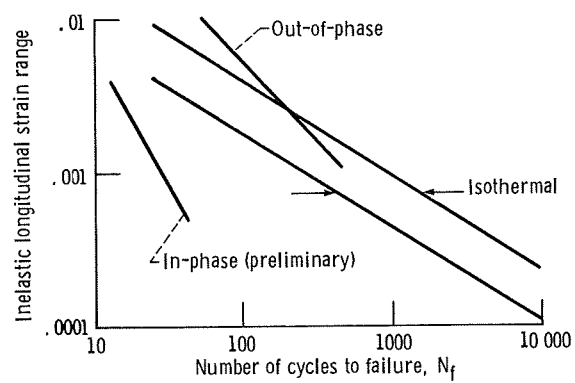
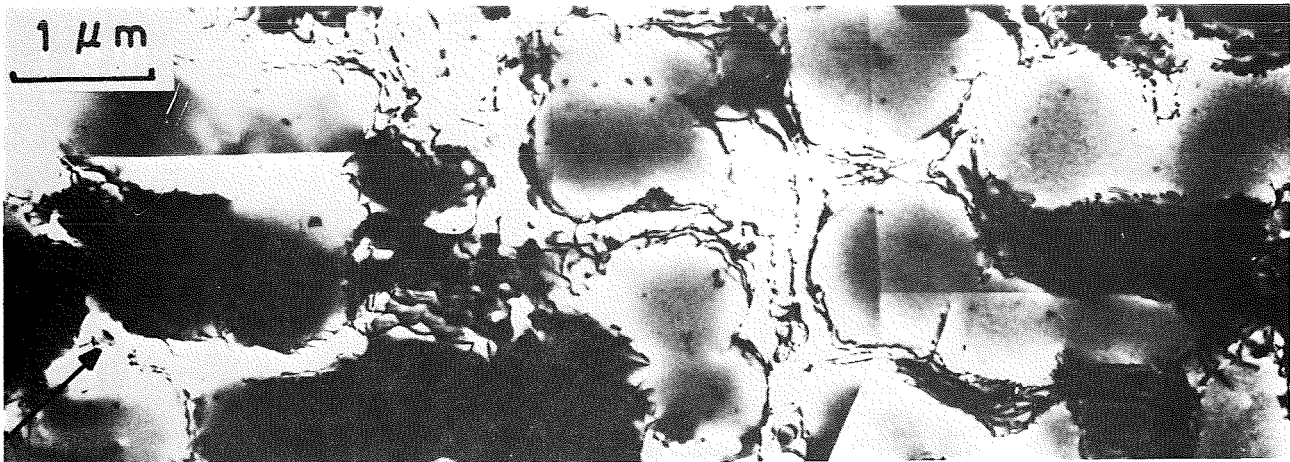
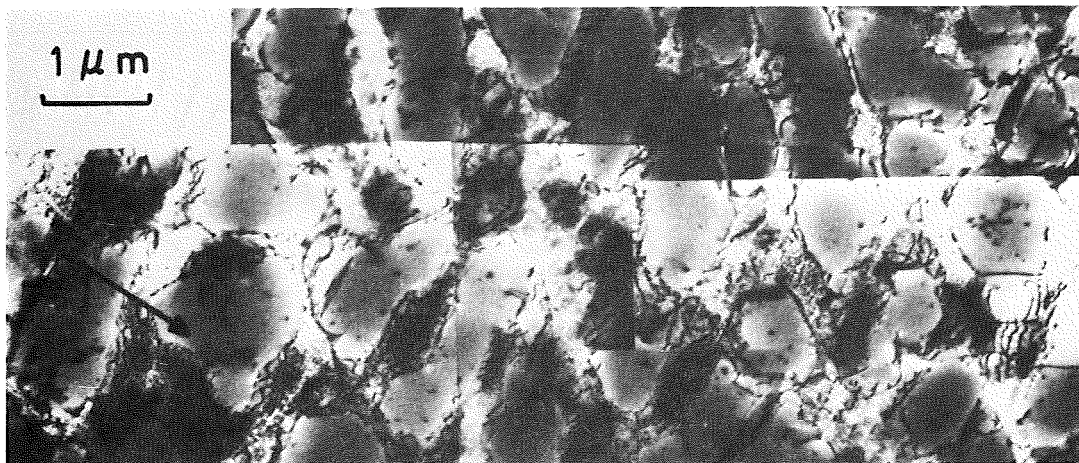


Figure 5. - Isothermal and thermomechanical fatigue results for B-1900+Hf cycles between 483 and 871 °C (Halford and McGaw, ref. 9).

ORIGINAL PAGE IS
OF POOR QUALITY



(A) IN-PHASE.



(B) OUT-OF-PHASE.

FIGURE 6.- DISLOCATION CONFIGURATIONS IN B-1900+HF RESULTING FROM
THERMOMECHANICAL FATIGUE CYCLING (PELLOUX AND MARCHAND, REF. 10).

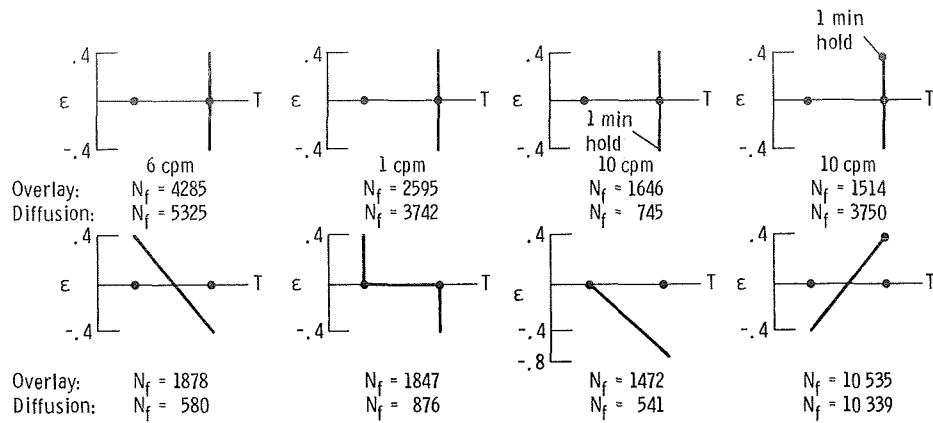
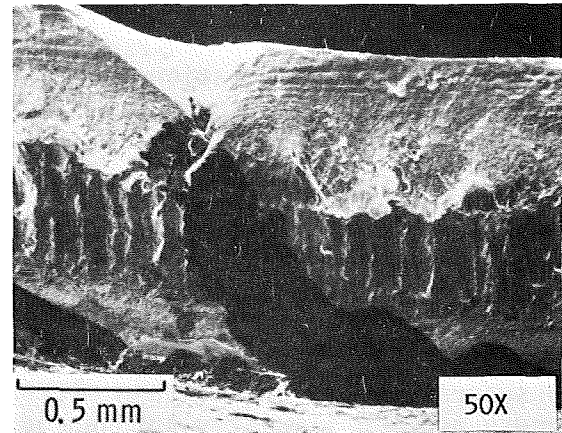
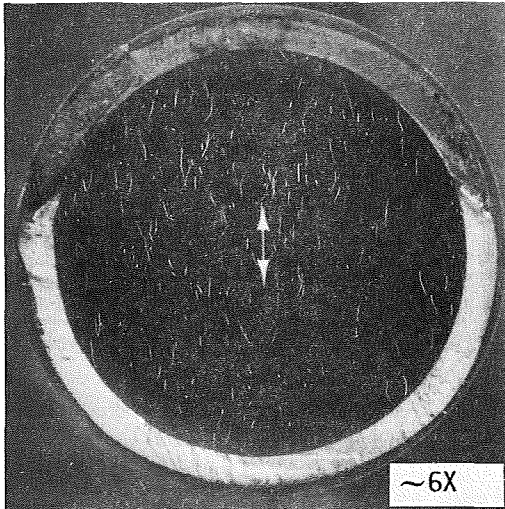
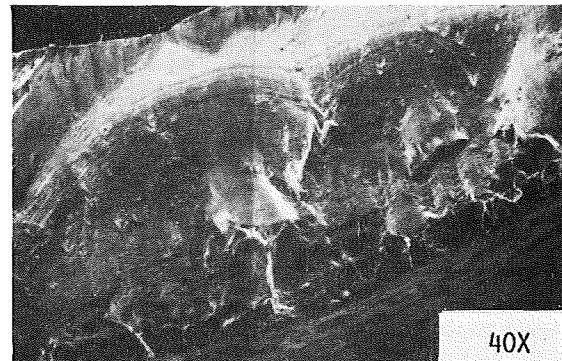
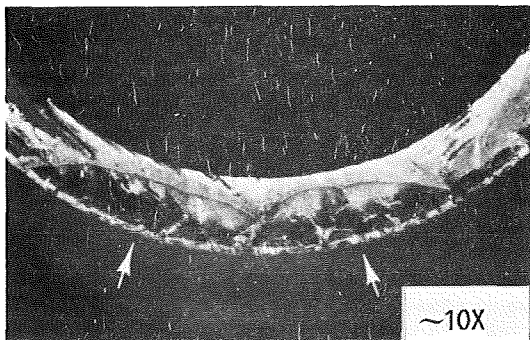


Figure 7. - Isothermal and thermomechanical fatigue results for coated single crystal PWA-1480. Maximum temperatures, 1038 °C (1900 °F); minimum temperatures, 427 °C (800 °F); strain range, 0.8 percent.

ORIGINAL PAGE IS
OF POOR QUALITY



(A) DIFFUSION COATING.



(B) OVERLAY COATING.

FIGURE 8.- ROLE OF COATING TYPE IN THERMOMECHANICAL FATIGUE CRACK INITIATION OF COATED SINGLE CRYSTAL PWA-1480.

1. Report No. NASA TM-87331 USAAVSCOM-TR-86-C-7		2. Government Accession No.		3. Recipient's Catalog No.	
4. Title and Subtitle Micromechanisms of Thermomechanical Fatigue - A Comparison With Isothermal Fatigue				5. Report Date	
				6. Performing Organization Code 505-63-11	
7. Author(s) Robert C. Bill				8. Performing Organization Report No. E-3075	
				10. Work Unit No.	
9. Performing Organization Name and Address NASA Lewis Research Center and Propulsion Directorate, U.S. Army Aviation Research and Technology Activity - AVSCOM, Cleveland, Ohio 44135				11. Contract or Grant No.	
				13. Type of Report and Period Covered Technical Memorandum	
12. Sponsoring Agency Name and Address National Aeronautics and Space Administration Washington, D.C. 20546 and U.S. Army Aviation Systems Command, St. Louis, Mo. 63120				14. Sponsoring Agency Code	
15. Supplementary Notes Prepared for the International Spring Conference "Fatigue at High Temperatures," sponsored by the Societe Francaise de Metallurgie, Paris, France, June 9-11, 1986.					
16. Abstract Thermomechanical Fatigue (TMF) experiments were conducted on Mar-M 200, B-1900, and PWA-1480 (single crystal) over temperature ranges representative of gas tur- bine airfoil environments. The results were examined from both a phenomenolog- ical basis and a micromechanistic basis. Depending on constituents present in the superalloy system, certain micromechanisms dominated the crack initiation process and significantly influenced the TMF lives as well as sensitivity of the material to the type of TMF cycle imposed. For instance, high temperature cracking around grain boundary carbides in Mar-M 200 resulted in short in-phase TMF lives compared to either out-of-phase or isothermal lives. In single crystal PWA-1480, the type of coating applied was seen to be the controlling factor in determining sensitivity to the type of TMF cycle imposed, out-of-phase lives being shortened compared to in-phase or isothermal lives if a coating that is brittle at the low temperature end of the cycle were applied. Micromechanisms of deformation were observed over the temperature range of interest to the TMF cycles, and provided some insight as to the differences between TMF damage mech- anisms and isothermal damage mechanisms. Finally, the applicability of various life prediction models to TMF results was reviewed. It was concluded that cur- rent life prediction models based on isothermal data must be modified before being generally applicable to TMF.Doc.					
17. Key Words (Suggested by Author(s)) Fatigue; High temperature; Superalloys; Thermomechanical fatigue; Crack initiation; Life prediction			18. Distribution Statement Unclassified - unlimited STAR Category 26		
19. Security Classif. (of this report) Unclassified		20. Security Classif. (of this page) Unclassified		21. No. of pages	
				22. Price*	

National Aeronautics and
Space Administration

Lewis Research Center
Cleveland, Ohio 44135

Official Business
Penalty for Private Use \$300

SECOND CLASS MAIL

ADDRESS CORRECTION REQUESTED



Postage and Fees Paid
National Aeronautics and
Space Administration
NASA-451

NASA
